

An experimental and theoretical approach to the study of the properties of parabanic acid and related compounds: synthesis and crystal structure of diethylimidazolidine-2-selone-4,5-dione

Massimiliano Arca, Francesco Demartin, Francesco A. Devillanova, Francesco Isaia, Francesco Lelj, Vito Lippolis, and Gaetano Verani

Abstract: The syntheses of the first examples of selenoparabanic acid derivatives (dialkylimidazolidine-2-selone-4,5-dione, $3e^R$, R = Me, Et, Bu) are presented along with the X-ray crystal structure determination of $3e^{Et}$. To gain an insight in the properties of parabanic acid derivatives on the basis of their electronic structures, we report the results of comparative hybrid-DFT calculations performed on parabanic, thioparabanic, and selenoparabanic acids ($3a^H$, $3b^H$, and $3e^H$) and on their *N,N'*-dimethyl derivatives ($3a^{Me}$, $3b^{Me}$, and $3e^{Me}$). Calculations show that the different nature of the frontier orbitals of $3a^R$ compared to those of $3b^R$ and $3e^R$, might account for the different reactivities of these compounds. Moreover, the weak donor character of $3b^R$ and $3e^R$ towards molecular di-iodine, estimated by FT-Raman measurements is in agreement with the calculated NBO-charge distribution.

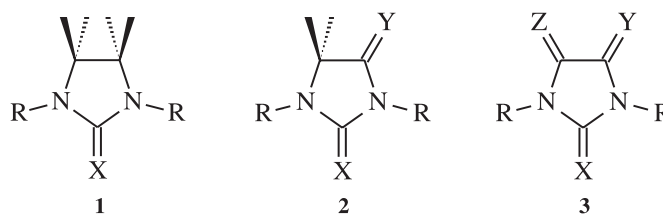
Key words: selenation, selenoparabanic derivatives, crystal structure, DFT calculations.

Résumé : Les synthèses des premiers exemples des dérivés de l'acide sélénoparabanique sont présentés avec la structure des rayons X du composé $3e^{Et}$. Pour mieux comprendre les propriétés des dérivés de l'acide parabanique sur la base de leurs structures électroniques, nous reportons les résultats des calculs comparatifs hybride-DFT effectués sur les acides parabanique, thioparabanique et sélénoparabanique ($3a^H$, $3b^H$ et $3e^H$) et sur les leurs dérivés *N,N'*-diméthylés ($3a^{Me}$, $3b^{Me}$ et $3e^{Me}$). Les calculs montrent que la différente nature des orbitales de frontière de $3a^R$ comparés avec ceux de $3b^R$ et $3e^R$ pourrait expliquer les différentes réactivités de ces composés. De plus, le faible caractère de donneur de $3b^R$ et $3e^R$ vers le iode moléculaire, évalué au moyen des mesures FT-Raman, est en accord avec la distribution des charges NBO.

Mots clés : Sélénation, dérivés de l'acide sélénoparabanique, structure cristalline, calculs DFT.

Introduction

For more than twenty years, our research group has dealt with the synthesis, characterization, and study of the coordination properties of imidazolidine derivatives containing one or two *exo*-chalcogen atoms (**1** and **2** respectively) (1, 2).



Received March 30, 2000. Published on the NRC Research Press website on August 15, 2000.

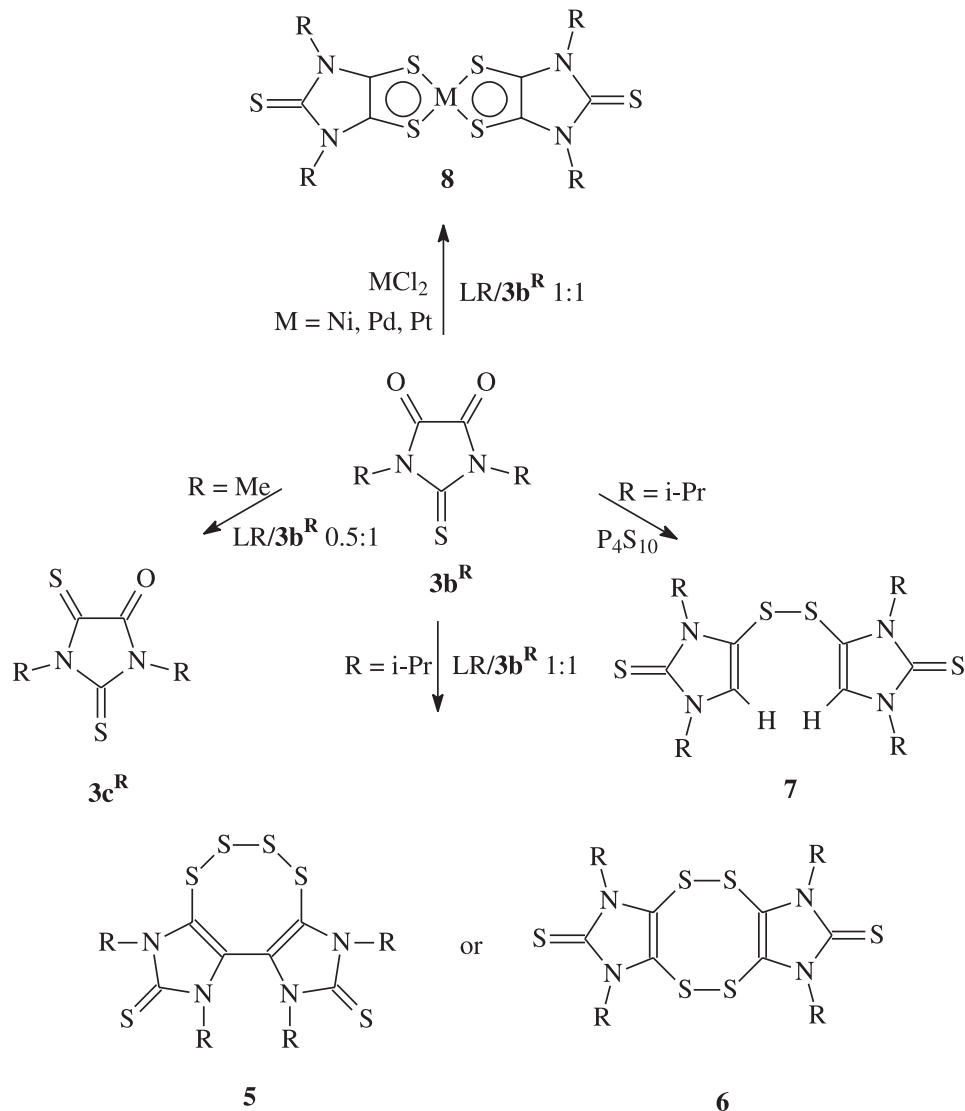
M. Arca,¹ F.A. Devillanova, F. Isaia, V. Lippolis,¹ and G. Verani. Dipartimento di Chimica Inorganica e Analitica, SS 554 bivio Sestu, 09042 Monserrato-Cagliari, Italy.

F. Demartin. Dipartimento di Chimica Strutturale e Stereochimica Inorganica, Via G. Venezian 21, 20133 Milano, Italy.

F. Lelj. Dipartimento di Chimica, Via N. Sauro 85, 85100 Potenza, Italy.

¹Authors to whom correspondence may be addressed. MA: Telephone: +39-070-675-4467/83. Fax: +39-070-675-4456. e-mail: marca@vaxca1.unica.it. VL: e-mail: lippolis@unica.it.

As a natural evolution of this research, we have turned our attention to trichalcogen-substituted imidazolidine derivatives **3**, with the aim of synthesizing dischotic metal complexes having a highly delocalized π -system for the preparation of unidimensional conducting materials. Among all the possible compounds (X, Y, Z = O, S, Se; R = H, alkyl, or aryl groups), only the syntheses of $3a^R$ (X = Y = Z = O, R = H (parabanic acid), alkyl, or aryl groups), (3, 4) $3b^R$ (X = S, Y = Z = O, R = H (thioparabanic acid), alkyl or aryl groups) (3) and $3c^R$ (Z = O, X = Y = S, R = Me, dithioparabanic acid derivatives) (5, 6) were reported in the literature. No other member of the possible compounds in this class has

Scheme 1. Reactivity of $3b^R$ towards Lawesson's reagent (LR) and P_4S_{10} in refluxing toluene.

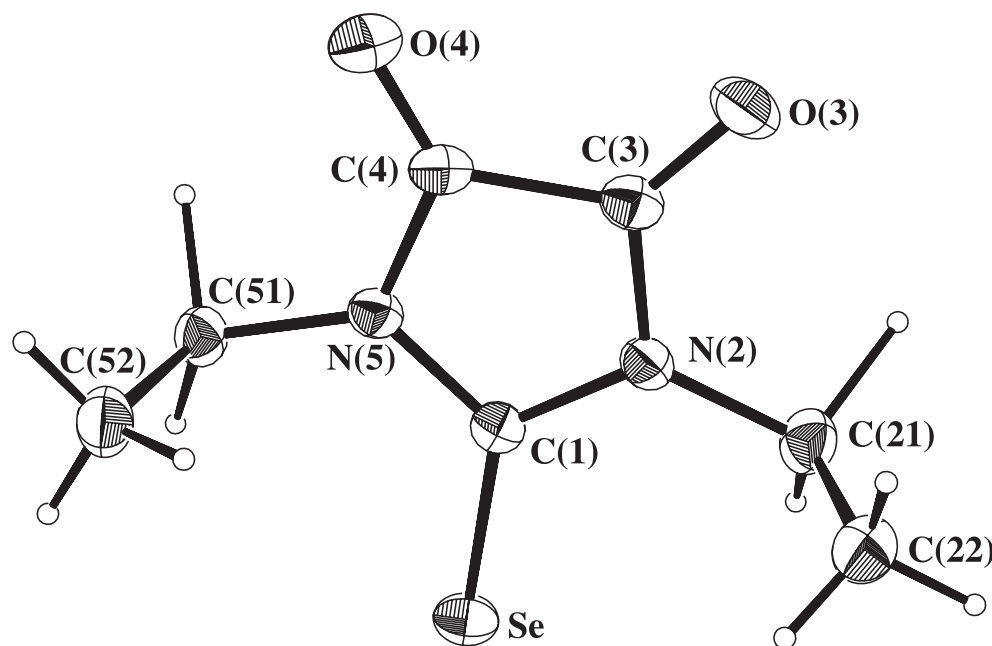
been synthesized and isolated so far. This seems to be in agreement with the alleged instability reported in the literature for five-membered cyclic dithioxamides, (**7**) which is probably also valid for diselenooxamides. However, the coordination chemistry of these compounds is completely unexplored, with the only exception of $3a^R$ ($R = C_6H_5NHCH_2$), for which at any rate just the NH groups seem to be responsible for the coordination to Co(II), Ni(II), and Cu(II) (**8**). This poverty of data seems to be due to the poor coordination abilities of the chalcogen donor atoms in **3**, rather than to a lack of interest for these compounds by the scientific community.

Many studies (**5**, **9**, **10**, **11**) have been carried out on the sulphuration reaction of $3a^R$ and $3b^R$ with P_4S_{10} and Lawesson's reagent (LR) (**12**) because this reaction represents a possible direct method for synthesizing trithione derivatives $3d^R$ ($X = Y = Z = S$). In particular, while the reaction of $3b^R$ with LR in a 1:0.5 ratio leads to $3c^R$ (Scheme 1, $R = Me$) (**5**) and in a 1:1 ratio to both 4,5,6,7- and 4,5,9,10-tetrathiocino compounds (**5** and **6**, respectively), (**9**, **10**) the reaction with P_4S_{10} leads to bis(1,3-dialkyl-2-

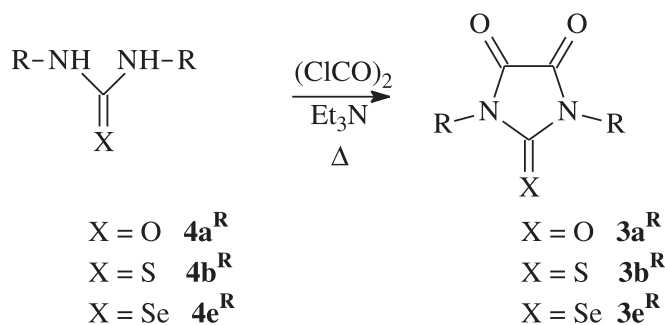
thioxoimidazolin-4-yl)disulfide (**7**, alkyl = *i*-Pr, see Scheme 1) (**10**). When the sulphuration of $3b^R$ with LR is carried out in presence of metal powder or salts, (**13**) the corresponding $[M(R_2timdt)_2]$ neutral complexes (**8**) can be obtained ($M = Ni, Pd, Pt$), where R_2timdt is the monoreduced anion of $3d^R$ (**11**, **14**). Complexes **8** represent a brand new class of metal dithiolenes characterized by a very large π -delocalization.

So far, no type **3** compounds containing a Se atom have been reported. In the present paper the synthesis and characterization of imidazolidine-2-selone-4,5-diones having methyl ($3e^{Me}$), ethyl ($3e^{Et}$), and butyl ($3e^{Bu}$) substituents is reported along with the single crystal X-ray structure of $3e^{Et}$. Analogously to $3b^R$, the sulphuration reaction of $3e^R$ (synthesized by us according to the method reported here and donated to the authors to study the reactivity of these compounds towards LR) leads again to tetrathiocino analogues (**15**). By carrying out the sulphuration reaction for longer times, the exocyclic selenium atoms can be replaced by sulphur atoms and move into the octa-membered ring (**15**).

Fig. 1. View of the molecular structure of compound $3e^{Et}$ with the numbering scheme adopted. Displacement ellipsoids are drawn at the 30% probability.



Scheme 2. Synthesis of parabanic, thioparabanic, and selenoparabanic acid derivatives from the corresponding ureas, thioureas, and selenoureas.



To rationalize the different chemical behavior of $3a,b,e^R$, especially as far as regarding sulphuration and coordinating ability, we performed hybrid-DFT (16, 17) calculations on $3a^H$, $3b^H$, and $3e^H$ and their methylated derivatives ($3a^{Me}$, $3b^{Me}$, and $3e^{Me}$).

Moreover, the donor properties of imidazolidine-2-selone-4,5-diones towards molecular di-iodine have been explored by electronic and FT-Raman spectroscopy, and the weakness of the interaction has been explained on the basis of the NBO-charge distribution.

Results and discussion

Synthetic aspects

The syntheses of $3a^R$ and $3b^R$ have long since been reported, (3, 4) and consist of a cyclization reaction between the corresponding ureas $4a^R$ or thioureas $4b^R$ and dicyanogen (the resulting 4,5-diiminoimidazolidine-2-one is hydrolyzed with diluted HCl) or oxalyl chloride (Scheme 2) (3). To prepare selenoparabanic acid derivatives ($3e^R$), the

substitution of the exocyclic sulphur atom of $3b^R$ with selenium was first attempted without encouraging results by the standard method for replacing S with Se in the $>C=S$ bond, i.e., addition of MeI to $>C=S$ to form the corresponding substituted *S,N,N'*-isothiuronium iodide and subsequent attack to the cation with HSe^- (18). More satisfactory results were achieved by reacting oxalyl chloride and disubstituted selenoureas $4e^R$ (Scheme 2, R = Me, Et, Bu), which can easily be prepared in good yields by the above method.

X-ray crystallography

A view of the crystal structure of $3e^{Et}$ is shown in Fig. 1. Table 1 shows a comparison of the interatomic distances with those of $3a^H$, which is the only other type 3 compound structurally characterized so far (19, 20, 21). The imidazolidine ring displays similar features in both cases, with a slight lengthening of the N(2)—C(3) and N(5)—C(4) bonds and a slight shortening of N(2),N(5)—C(1) bonds, due to an increase in the conjugation of the lone pairs of the two nitrogen atoms towards C(1) in the presence of the Se atom. The five-membered ring is rigorously planar and the atoms Se, O(3), O(4), C(21), and C(51) lie essentially in the plane of the ring (maximum deviation observed 0.05 Å for Se).

Theoretical calculations

With the aim of understanding the effect of the nature of the chalcogen atom bound to the C(1) on the electronic and structural features, and possibly on the reactivity of the molecules of type 3, DFT (16, 17) calculations have been performed on the molecules reported in Scheme 3. According to the good results recently found on $[M(R_2timdt)_2]$ dithiolenes **8**, (11) hybrid BECKE3LYP functional (22, 23) and Schafer, Horn, and Ahlrichs' (24) pVDZ basis set have been used throughout in the calculations. The Khon–Sham frontier orbital energies are reported in Fig. 2 and a perspective

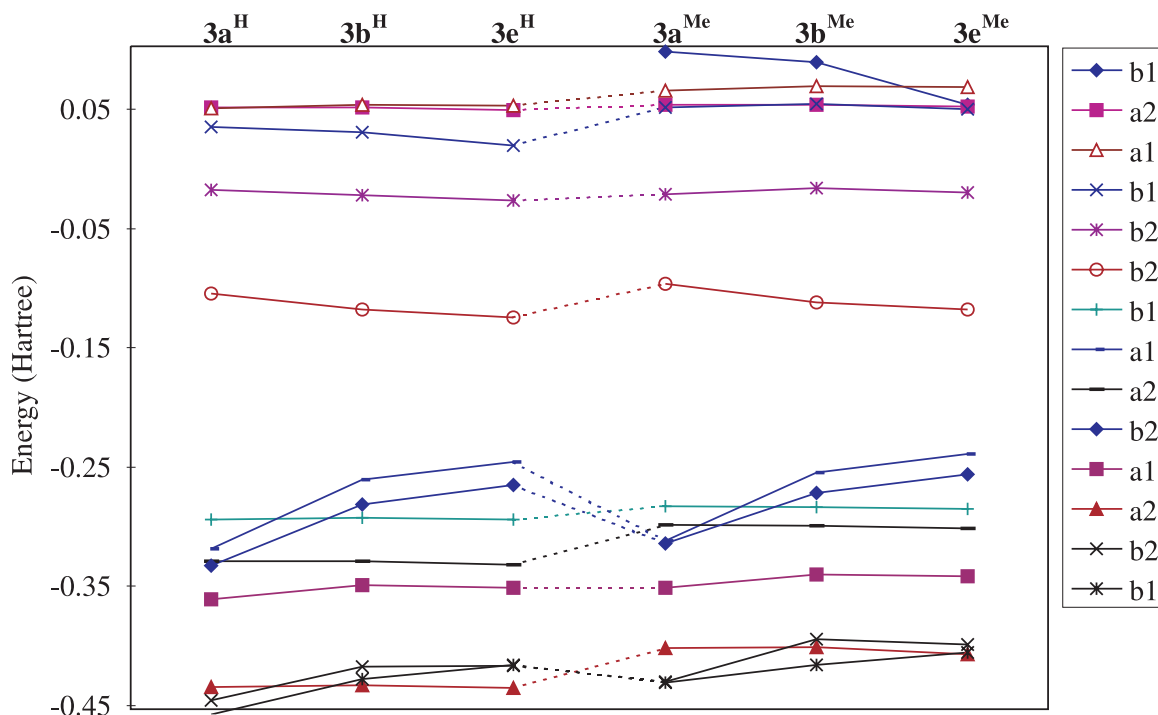
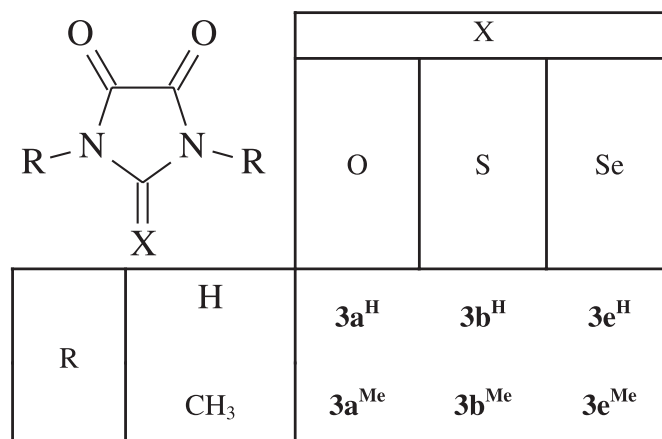
Table 1. Selected interatomic distances (Å) and angles (°) for compounds **3e^{Et}** and **3a^H**.^a

Interatomic distances (Å)	3e^{Et}	3a^H
C(1)—X ^b	1.785(3)	1.203
C(3)—O(3)	1.205(3)	1.213
C(4)—O(4)	1.192(3)	1.205
C(1)—N(2)	1.364(3)	1.399
C(1)—N(5)	1.387(3)	1.396
C(3)—N(2)	1.383(4)	1.362
C(4)—N(5)	1.381(3)	1.360
C(3)—C(4)	1.530(4)	1.551
Angles (°)		
C(1)-N(2)-C(3)	111.5(2)	111.6
C(1)-N(5)-C(4)	110.7(2)	111.3
Se-C(1)-N(2)	126.0(2)	126.6
Se-C(1)-N(5)	125.6(2)	126.1
N(2)-C(1)-N(5)	108.4(2)	107.3
O(3)-C(3)-N(2)	127.6(3)	128.8
O(3)-C(3)-C(4)	127.8(3)	129.1
N(2)-C(3)-C(4)	104.5(2)	104.8
N(5)-C(4)-C(3)	104.8(2)	105.0
O(4)-C(4)-N(5)	127.1(3)	126.1
O(4)-C(4)-C(3)	128.1(3)	126.2

^aValues taken from ref. (20) accounting for rigid-body libration corrections.

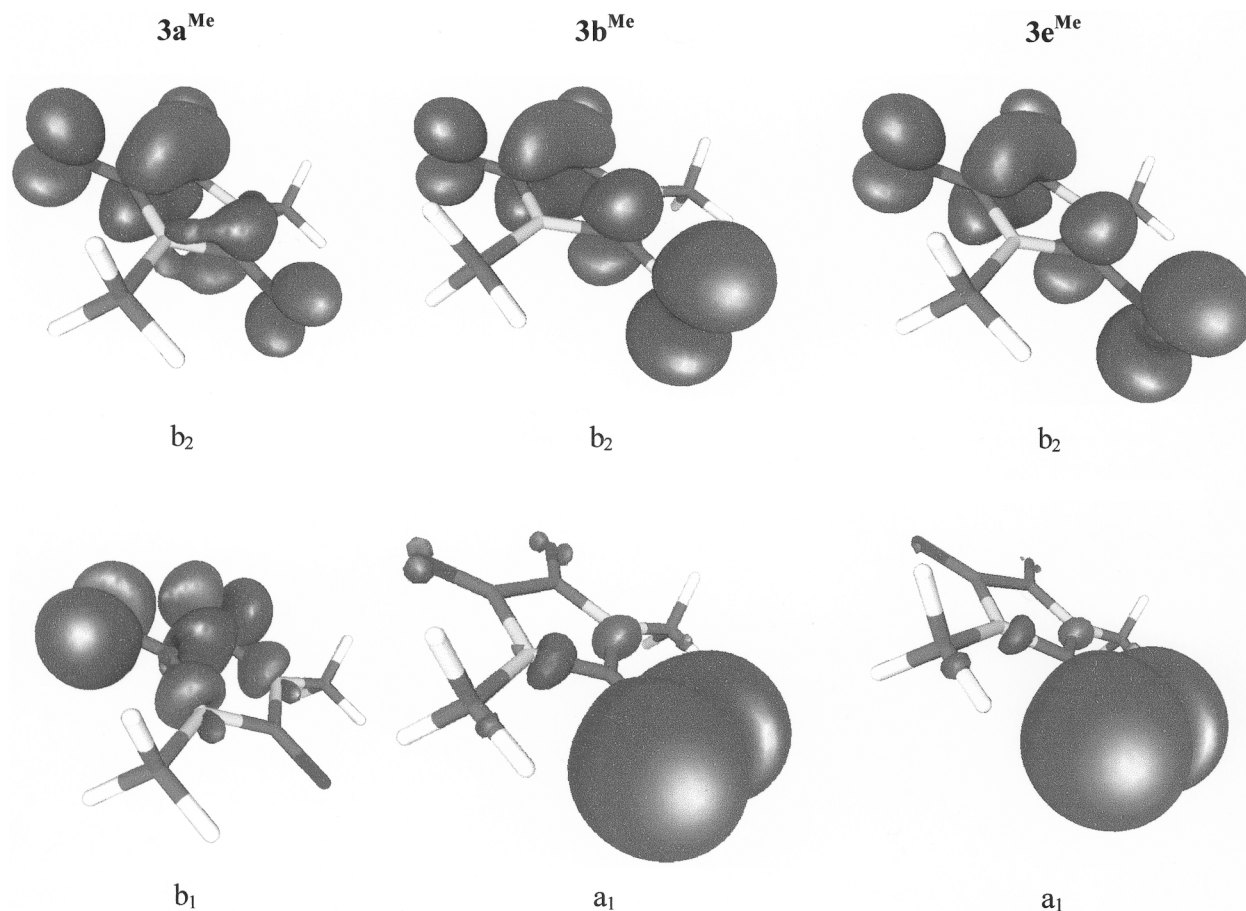
^bAtom numbering as in Fig. 1. X = O for **3a^H**, Se for **3e^{Et}**.

drawing of HOMOs and LUMOs for compounds **3a**, **b**, **e^{Me}** is shown in Fig. 3. The energies of the two highest occupied orbitals (HOMO and HOMO-1) in **3a^R** are swapped with respect to those calculated for **3b^R** and **3e^R** (R = H, Me). As a consequence, while the HOMO in thio- and seleno-

Fig. 2. Calculated Kohn–Sham orbital energies (Hartree) of the frontier orbitals for compounds reported in Scheme 3. The box shows the representations of molecular orbitals in the C_{2v} point group.**Scheme 3.** Naming of the model compounds for DFT-calculations.

derivatives is an a_1 lone pair centred on the respective chalcogen atom, the HOMO in parabanic acid derivatives is made up of the $2p$ atomic orbitals of O(3) and O(4) lying on the molecular plane, and of the $2s$ and $2p$ atomic orbitals of nitrogen and carbon atoms combining to form a $p\sigma$ bonding molecular orbital extending over the N(2)-C(3)-C(4)-N(5) framework and belonging to the b_1 representation. The different nature of the HOMOs of **3a^R** compared to those of **3b^R** and **3e^R** might be responsible for the different reactivities

Fig. 3. HOMOs (bottom row) and LUMOs (upper row) drawings for compounds $3a^{\text{Me}}$, $3b^{\text{Me}}$, and $3e^{\text{Me}}$.



of these substrates, in particular as far as the sulphuration is concerned.

To ascertain whether the change in the nature of the HOMO only depends upon the nature of the X atom, and is common to all systems containing the $-\text{NH}-\text{C}(\text{X})-\text{NH}-$ moiety, the same type of calculations (BECKE3LYP/Ahlich basis set) have been performed on $4a^{\text{H}}$, $4b^{\text{H}}$, and $4e^{\text{H}}$ (optimized bond lengths and angles: C—N, 1.375, 1.365, 1.351 Å; C=X: 1.228, 1.669, 1.837 Å; N—C—N: 115.29, 115.01, 116.54°) and on $4a^{\text{Me}}$, $4b^{\text{Me}}$, and $4e^{\text{Me}}$ (with the substituents arranged in a *cis-cis* configuration, to preserve the C_{2v} symmetry. Optimized bond lengths and angles: C—N, 1.378, 1.366, 1.358 Å; C=X: 1.232, 1.680, 1.846 Å; N—C—N: 114.64, 113.40, 113.81°). The calculated geometries for $4b^{\text{Me}}$ can be compared with the experimental bond lengths and angles determined by X-ray diffraction for $4b^{\text{Et}}$, $4b^{\text{i-Pr}}$, and $4b^{\text{Ph}}$ (C—N, 1.316(4), 1.332(2), 1.384(5) Å; C=X: 1.707(3), 1.711(2), 1.681(5) Å; N—C—N: 117.3(3), 118.3(1), 113.9(4)°, respectively (25)). The best agreement is found with $4b^{\text{Ph}}$, possibly because $4b^{\text{Et}}$ and $4b^{\text{i-Pr}}$ adopt a *cis-trans* configuration in the solid state, which leads to the formation of two-dimensional layers of thiourea derivatives. At any rate, as far as regards the N—C and the $> \text{C}=\text{S}$ moieties, it should be remarked that bond lengths calculated in $4b^{\text{Me}}$ correspond well to the unweighted mean values determined in thioureas from diffraction techniques (1.346 and 1.681 Å, respectively) (26). Interestingly, while all compounds with R = H, have the same kind of HOMOs, consisting in the lone

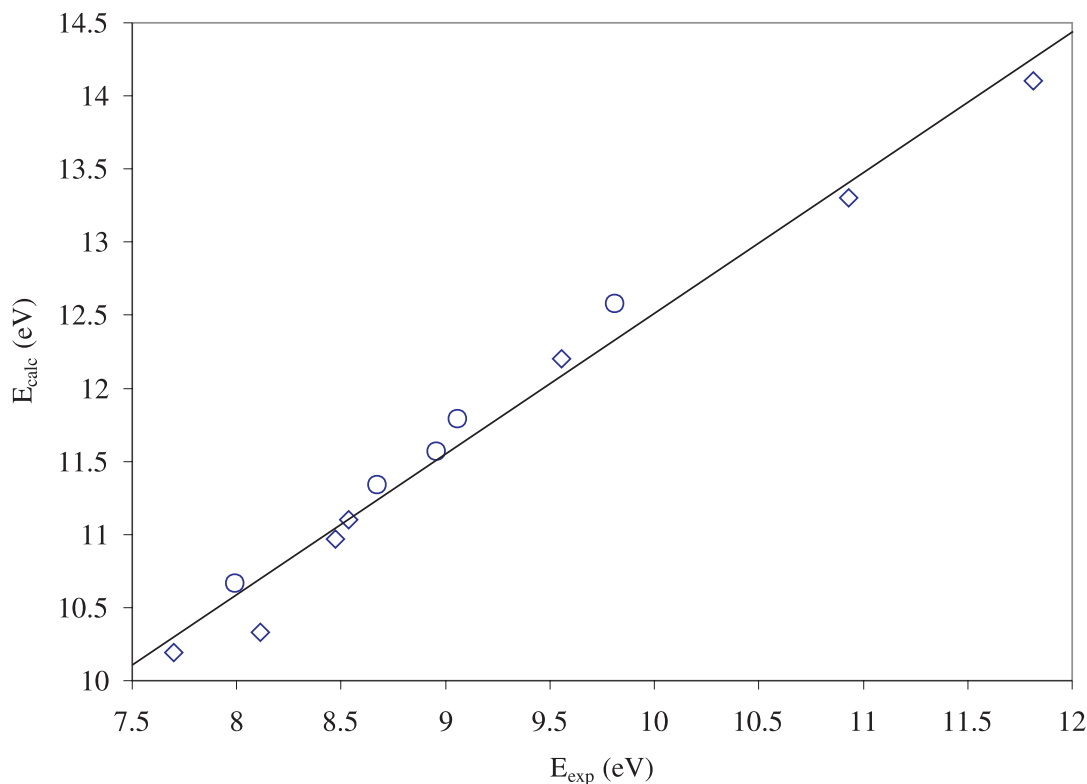
pair of the chalcogen atom lying on the molecular plane, as found in $3b^{\text{R}}$ and $3e^{\text{R}}$, those with R = Me show the same level inversion between HOMO and HOMO-1 calculated for $3a^{\text{R}}$. The NBO-charges (N: -0.87, -0.80, -0.80, -0.69, -0.63, -0.63; C: +0.84, +0.29, +0.25, +0.86, +0.32, +0.27; X: -0.68, -0.25, -0.26, -0.70, -0.28, -0.26 e for $4a^{\text{H}}$, $4b^{\text{H}}$, $4e^{\text{H}}$, $4a^{\text{Me}}$, $4b^{\text{Me}}$, $4e^{\text{Me}}$, respectively) and the analysis of the bond order demonstrate that the nitrogen lone pairs are conjugated with the $> \text{C}=\text{X}$ system in an order that increases on passing from $4a^{\text{R}}$ to $4e^{\text{R}}$ (N lone pair occupancies: 1.80, 1.76, 1.73, 1.77, 1.72, 1.70 e for $4a^{\text{H}}$, $4b^{\text{H}}$, $4e^{\text{H}}$, $4a^{\text{Me}}$, $4b^{\text{Me}}$, and $4e^{\text{Me}}$, respectively). At any rate, the charge distributions in $4b^{\text{H,Me}}$ and $4e^{\text{H,Me}}$ are very similar, and sensibly differ from those calculated for $4a^{\text{H,Me}}$.

Returning to compounds of type 3, the b_2 LUMOs are π^* molecular orbitals formed by the $2p$ and $3p$ orbitals of all the endocyclic carbon atoms and of the exocyclic chalcogen atom. Some selected optimized bond lengths and angles are reported in Table 2. The agreement between the calculated parameters and experimental data available for $3a^{\text{H}}$ (20) and for $3e^{\text{Et}}$ (Table 1) is quite good, with differences within 2%, probably due to solid state effects. We have recently pointed out (11, 14) that although Koopmans' (27) theorem is not valid in DFT, a linear correlation can be found between the Kohn–Sham orbital energies and electronic properties such as molecular electronic transitions and redox potentials. Analogously, in this case a correlation between experimental photoelectron spectra (reported for $3a^{\text{H}}$ and $3a^{\text{Me}}$) (28) and

Table 2. Calculated bond lengths (Å) and angles (°) for model compounds reported in Scheme 3.

	3a^H	3b^H	3e^H	3a^{Me}	3b^{Me}	3e^{Me}
Bond lengths (Å)						
C(1)—X ^a	1.208	1.634	1.791	1.213	1.642	1.801
C(1)—N(2)	1.399	1.387	1.379	1.401	1.394	1.387
N(2)—C(3)	1.386	1.389	1.391	1.384	1.388	1.391
C(3)—O(3)	1.207	1.209	1.208	1.210	1.211	1.212
C(3)—C(4)	1.556	1.549	1.547	1.547	1.535	1.532
Angles (°)						
X-C(1)-N(2)	127.15	127.21	126.94	126.38	126.57	126.36
N(2)-C(1)-N(5)	105.70	105.58	106.11	107.24	106.86	107.28
N(2)-C(3)-C(4)	104.07	103.74	103.64	104.85	104.70	104.63
C(3)-C(4)-O(4)	127.61	128.17	128.39	127.94	128.52	128.70

^aAtom numbering as in Fig. 1. X = O for **3a^{H,Me}**, S for **3b^{H,Me}**, Se for **3e^{H,Me}**.

Fig. 4. Experimental ionization energies (eV, ref. (28)) vs. calculated Kohn–Sham orbital energies (eV) for **3a^H** (circles) and **3a^{Me}** (squares).

calculated Kohn–Sham eigenvalues can be found (Fig. 4 and Table 3). The shifts in the positions of the PES peaks found on passing from **3a^H** to **3a^{Me}** due to methylation show the same trend for both experimental and calculated energies (Fig. 5a). Moreover, a new evaluation of the energy values reported for **3a^{Me}**, previously estimated with the help of the results of CNDO/s-CI calculations, (28) leads to a better agreement (Fig. 5b). The very good correlation between the shifts in the ionization energies and in the calculated Kohn–Sham orbital energies between methylated and unmethylated parabenic acid indicates that the attribution of π -orbitals perpendicular to the molecular plane (such as HOMO-1 (a_1), HOMO-3 (b_2), and HOMO-5 (a_2) for **3a^{Me}**), in which methyl groups are able to participate sensibly, is correct. As far as

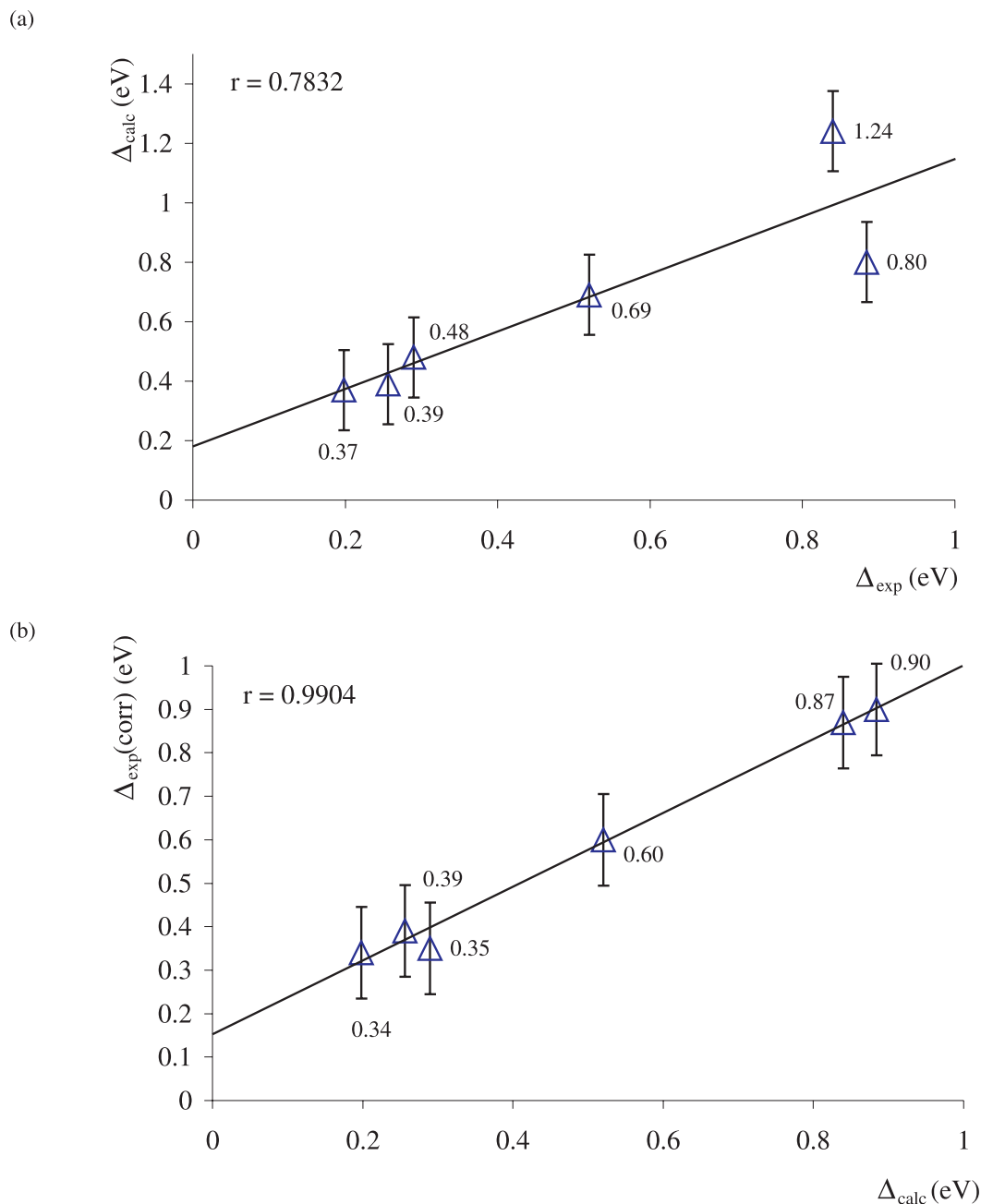
Table 3. Calculated Kohn–Sham orbital energies (eV) and experimental ionization energies^a (eV) for **3a^H** and **3a^{Me}**.

	Calculated eigenvalues (eV)		Exp. ionization energies (eV) ^b		
	3a^H	3a^{Me}	3a^H	3a^{Me}	
b_1	7.99	7.70	10.67	10.19	(10.32)
a_1	8.67	8.47	11.34	10.97	(10.70)
a_2	8.95	8.11	11.57	10.33	(11.00)
b_2	9.06	8.54	11.79	11.10	(11.19)
a_1	9.81	9.55	12.58	12.19	(12.28)
a_2	11.82	10.93	14.10	13.30	(13.20)

^aLiterature values obtained from PES data (ref. (28)).

^bIn parentheses new energy values extrapolated from data reported in ref. (28) are reported for **3a^{Me}**.

Fig. 5. Correlation and SDs between calculated and experimental shifts Δ (eV) found in the PES of $3a^H$ and $3a^{Me}$. As experimental data both literature (a, ref. (28)) and newly extrapolated data (b) have been used.



the charge distribution is concerned, NBO (29) charges (which are more reliable (30) than Mulliken charges²) are summarized in Table 4. For $3a^{H,Me}$ net negative charges are found on all exocyclic O atoms with similar values. In the case of $3b^{H,Me}$ and $3e^{H,Me}$, while O(3) and O(4) show very similar NBO-charges, almost identical to those calculated for $3a^{H,Me}$, the S and Se atoms bound to C(1) are almost neutral. Correspondingly, the C(1) atoms in $3a^H$ and $3a^{Me}$ bear a more positive charge than those in $3b^{H,Me}$ and $3e^{H,Me}$. While the charge distribution on C(1) and X (X = O, S, and

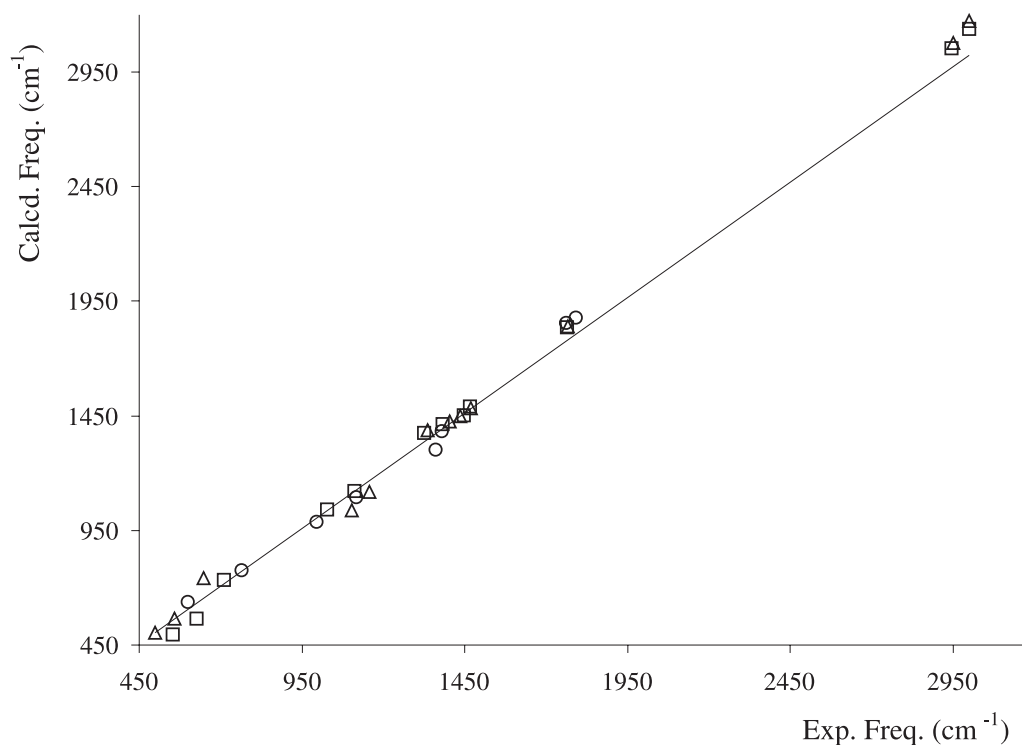
Se for $3a$, $3b$, and $3e$, respectively) strongly depends on the nature of the X atom, in agreement with the trend of the softness of X, the remaining atoms in the molecule show very similar charge distributions. Actually, the almost neutral charges on the sulphur and selenium atoms in $3b^{H,Me}$ and $3e^{H,Me}$, respectively suggest a very weak donor character for these compounds towards Lewis acids, such as halogen or interhalogen compounds, compared to that of compounds **1** (31, 32, 33) and **2** (34, 35). This is in accordance with the fact that we have been unable to measure reliable formation

²Mulliken charges for X, C(1), N(2,5), C(3,4), O follow: $3a^H$: -0.383, +0.240, -0.209, -0.004, -0.027; $3b^H$: -0.166, +0.093, -0.200, -0.011, -0.011, -0.042; $3e^H$: +0.174, -0.286, -0.175, -0.013, -0.047; $3a^{Me}$: -0.068, +0.112, -0.157, +0.009, -0.033; $3b^{Me}$: -0.136, +0.106, -0.110, +0.006, -0.034; $3e^{Me}$: +0.155, -0.244, -0.087, +0.007, -0.032 e.

Table 4. NBO-charges (e) for compounds reported in Scheme 3.^a

Atom	3a^H	3b^H	3e^H	3a^{Me}	3b^{Me}	3e^{Me}
X	-0.573	-0.044	+0.005	-0.592	-0.070	-0.018
C(1)	0.875	+0.249	+0.186	+0.892	+0.277	+0.211
N(2),N(5)	-0.710	-0.660	-0.655	-0.550	-0.505	-0.504
C(3),C(4)	0.636	+0.631	+0.627	+0.647	+0.643	+0.641
O(3),O(4)	-0.519	-0.518	-0.515	-0.532	-0.529	-0.526

^aAtom numbering as in Fig. 1. X = O for **3a^{H,Me}**, S for **3b^{H,Me}**, Se for **3e^{H,Me}**.

Fig. 6. Experimental vs. calculated mid-IR frequencies (450–3 200 cm⁻¹) for **3a^H** (circles), **3b^{Me}** (triangles), and **3e^{Me}** (squares).

constants of the adduct formed between **3b^R** and **3e^R** with molecular di-iodine. In fact, when the donor–acceptor interaction is very weak, a spectrophotometric approach (36) is not well-suited, since it is not possible to prepare solutions having a sufficiently high value of the saturation fraction (37, 38). In addition, in this particular class of compounds, an absorption band ($\lambda_{\max} = 520$ nm, $\epsilon = 215$ M⁻¹ cm⁻¹ for **3e^{Me}**) near to the visible band of molecular di-iodine and a stronger band ($\lambda_{\max} = 350$ nm, $\epsilon = 16\,900$ M⁻¹ cm⁻¹ for **3e^{Me}**) which falls just where the adduct CT-band should appear, make further unreliable simultaneous determinations of the K and ϵ values of the adduct. Nevertheless, it is possible to have a rough estimation of the enthalpy value for the reaction of the 1:1 adduct formation from the lowering of the FT-Raman frequency for the I–I stretching (in methylene chloride solution ν_{I-I} falls at 209 cm⁻¹ for free I₂ and at 182, 185, and 185 cm⁻¹ in the adducts with **3e^{Me}**, **3e^{Et}**, and **3e^{Bu}**, respectively). From the lowering of the ν_{I-I} value, a ΔH value of about -15 KJ mol⁻¹ can be estimated. This value corresponds to a very weak interaction, and well agrees with the low charges calculated on the S and Se atoms in **3b^R** and **3e^R**. As far as compounds of type **3b** are concerned, an adduct having an elemental analysis indicating a stoichio-

metry **3b^R•I₂** (R = Et) has been isolated in the solid state from CHCl₃ solutions. The very low interaction is confirmed by the position of the Raman band (180 cm⁻¹). In fact, their quick decomposition, with ejection of diiodine under the X-ray beam, prevented the crystal structure characterization of this adduct. A low-temperature determination has not been performed because of the scarce diffraction of the crystals.

Vibrational spectroscopy

Finally, DFT calculations can be employed to understand the vibrational spectra of the examined compounds. Calculated harmonic frequencies and experimental values appear to be in fairly good agreement as far as regards the trend in the values of the frequencies and in their intensities. Figure 6 shows a graph reporting the correlation between the experimental FT mid-IR frequencies and the harmonic calculated frequencies for **3b^{Me}** and **3e^{Me}**. For the sake of comparison, the data regarding **3a^H** (39) are also reported. A comparison of the data available for all compounds allows to estimate an overall linear average scaling factor of 0.968. Furthermore, the results of our calculations allow to confirm or correct previous attributions based on an exclusively experimental basis. Thus, in Table 5 a comparison between

Table 5. Experimental IR-active frequencies (cm^{-1}) and calculated unscaled and scaled^a mid-IR frequencies (cm^{-1}), intensities (KM mol^{-1}), old attribution,^b and description of the vibrations for **3a^H**.

Attrib.	Exp. (cm^{-1}) ^a	Unscaled (cm^{-1})	Scaled (cm^{-1}) (sc. factor) ^b	Int. (KM mol^{-1})	Old attrib.	Description
1 b_2	595s	640	624 (0.975)	236	b_1	NH out of plane
2 b_2	755s	761	757 (0.995)	28	—	C-N str. + O-C(1)-N bend.
3 b_1	982s	989	984 (0.995)	27	b_1	C-N symm. + N-C-C bend
4 a_1	1125m	1095	1089 (0.995)	10	a_1	C-N str. + O-C(4,5)-N bend.
5 b_1	1360s	1304	1297 (0.995)	134	b_1	C-N str. + O-C(4,5)-N bend.
6 a_1	1380s	1385	1378 (0.995)	247	a_1	C-N symm. + O-C(1)-N bend.
7 b_1	1760vs	1855	1658 (0.942)	1056	a_1	C=O str. + Ring def.
8 a_1	1790s	1878	1769 (0.942)	108	b_1	C=O str. + C-C str.
9 a_1	3160s	3622	3213 (0.887)	182	a_1	NH unsymm. str.
10 b_1	3220s	3624	3214 (0.887)	34	b_1	NH symm. str.

^aRef. (39).^bScaling factors taken from ref. (40) according to the nature of the vibration.

the experimental (39) and the harmonic calculated mid-IR frequencies for **3a^H** is reported. To obtain a better agreement, the calculated spectra can be scaled by the transferable factors recently reported for a series of organic compounds, according to the nature of the vibrational mode (40). The new attributions generally confirm those previously reported (except for modes 1 and 2 in Table 5 and for the order of modes 7 and 8).

Conclusions

Among compounds of type **3**, only **3a^R**, **3b^R**, and **3c^R** were known, (3–6) and only **3a^H** was structurally characterized (19). Now, the synthesis of the first examples of selenoparabanic acid derivatives **3e^R** (R = Me, Et, Bu) and the single crystal X-ray structure of **3e^{Et}** are reported. The comparison with the structural features (20) of **3a^H** supports a higher degree of electron delocalization on the N(2)-C(1)(Se)-N(5) fragment. Hybrid-DFT (16, 17) calculations performed on the molecules **3a**, **b**, **e^R** (R = H, Me) confirm an increase in the electron delocalization on this fragment on passing from O to S and Se derivatives, and indicate a different composition of the HOMOs of **3a^R** compared to those of **3b**, **e^R**. This might explain the similar reactivities of the latter compounds compared to the former, in particular as far as regards sulphuration with Lawesson's reagent (9–11). Because of experimental difficulties, the donor character of the new compounds towards molecular di-iodine cannot be quantitatively explored by UV-vis spectroscopy (36), but FT-Raman spectroscopy allows to estimate a ΔH value of about -15 kJ mol^{-1} . Such a low value corresponds to a very weak donor character of compounds **3b**, **e^R** compared to the donor ability of compounds of type **1** and **2**. This is also in good agreement with the NBO-charge distributions.

Experimental section

All solvents and reagents were Aldrich products used as purchased. All reactions were carried out under dry nitrogen atmosphere. Elemental analyses were performed on a FISON EA-1108 CHNS-O instrument. FT IR spectra were recorded on a Bruker IFS55 spectrometer at room temperature, purging the sample cell with a flow of dried air. Polythene pellets with a mylar beam-splitter and polythene

windows ($500\text{--}100 \text{ cm}^{-1}$, resolution 2 cm^{-1}) and KBr pellets with a KBr beam-splitter and KBr windows ($4000\text{--}400 \text{ cm}^{-1}$, resolution 4 cm^{-1}) were used. FT-Raman spectra were recorded with a resolution of 4 cm^{-1} on a Bruker RFS100 FT-Raman spectrometer, fitted with an In-Ga-As detector (room temperature) operating with a Nd-YAG laser (excitation wavelength 1064 nm), with a 180° scattering geometry. Electronic spectra were recorded with a quartz cell of an optical path of 1 cm or with cells of an optical path of 0.1 cm in the attempt to determine formation constants, on a Varian Cary 5 spectrophotometer in CH_2Cl_2 solution at 20°C in a thermostated compartment. The ^1H NMR and ^{13}C NMR spectra were recorded on a Varian Unity Inova 400 operating at 400 and 100.5 MHz, respectively. Chemical shifts of compounds dissolved in CDCl_3 were referred to TMS used as an internal reference.

Procedures

Among the examined compounds (Scheme 3), **3a^H** is commercially available, while **3b^H**, **3a^{Me}**, and **3b^{Me}** have been prepared according to literature methods (3).

Synthesis of **3e^{Me}**, $\text{C}_5\text{H}_6\text{N}_2\text{O}_2\text{Se}$

Iodomethane (2.4 mL, 38.4 mmol) is added dropwise to a methyl alcohol solution (20 mL) of *N,N'*-dimethylthiourea (2 g, 19.2 mmol) and the resulting mixture is refluxed for 1 h and then cooled to 0°C . The *S,N,N'*-trimethylisothiuronium iodide, separated as a white solid (4.3 g, yield 90%), is dissolved in anhydrous methyl alcohol and reacted at room temperature for 15 h with an absolute ethyl alcohol solution of NaHSe freshly prepared from selenium powder (0.834 g, 10.57 mmol) and sodium borohydride (0.492 g, 13.01 mmol). The mixture is neutralized with diluted acetic acid, 25 mL of distilled water are added, and alcohols are removed under reduced pressure. The *N,N'*-dimethylselenourea **4e^{Me}** is extracted with methylene chloride and the solution dried over anhydrous sodium sulfate. Trimethylamine (2.26 mL, 16.3 mmol) and oxalyl chloride (0.78 mL, 8.9 mmol) are added dropwise at 0°C to a methylene chloride solution of **4e^{Me}** containing 8.9 mmol and the reaction mixture is stirred at room temperature for 1 h, washed with water, and the organic phase dried under reduced pressure. The product is purified by crystallization from an ethyl

alcohol–hexane solution. Yield 0.917 g, 55%, mp 119°C. UV–vis (CH₂Cl₂ solution) λ (nm) (ϵ , M⁻¹ cm⁻¹): 347 (6800), 518 (200). IR ν (cm⁻¹): 2948vw, 1760vs, 1664w, 1467m, 1446s, 1379vs, 1323vs, 1229m, 1109s, 1027w, 964w, 785m, 711m, 625m, 554m, 484s, 381m, 325m, 249m. ¹H NMR (400.0 MHz, CDCl₃, TMS) δ : 3.52 (s). ¹³C NMR (100.5 MHz, CDCl₃, TMS) δ : 186.24, 154.91, 30.07. Anal. calcd.(%): C 29.28, H 2.95, N 13.66; found: C 30.08, H 2.81, N 13.94.

Synthesis of 3e^{Et}, C₇H₁₀N₂O₂Se

3e^{Et} was synthesized following the route outlined for 3e^{Me}. Yield 1.658 g, 65%, mp 111°C. UV–vis (CH₂Cl₂ solution) λ (nm) (ϵ , M⁻¹ cm⁻¹): 350 (6200), 524 (200). IR ν (cm⁻¹): 2971w, 1766vs, 1454m, 1430m, 1396vs, 1242vs, 1117s, 1074m, 1049w, 1010vw, 901w, 875w, 641m, 367m, 488s, 441w, 395w, 325m, 247vw, 225w, 198w, 187w. ¹H NMR (400.0 MHz, CDCl₃, TMS) δ : 4.12 (q, 2H), 1.30 (t, 3H). ¹³C NMR (100.5 MHz, CDCl₃, TMS) δ : 184.48, 154.81, 38.89, 13.14. Anal. calcd. (%): C 36.06, H 4.32, N 12.28; found: C 36.84, H 4.72, N 12.28.

Synthesis of 3e^{Bu}, C₁₁H₁₈N₂O₂Se

3e^{Bu} was synthesized following the route outlined for 3e^{Me}. Yield 1.227 g, 70%. mp 35°C. UV–vis (CH₂Cl₂ solution) λ (nm) (ϵ , M⁻¹ cm⁻¹): 352 (5600), 525 (200). IR ν (cm⁻¹): 2960m, 2933w, 2874w, 1767vs, 1434m, 1395vs, 1291m, 1209s, 1164w, 1130m, 1089w, 1061w, 957vw, 703vw, 573w, 495m, 397 w, 300w, 249vw. ¹H NMR (400.0 MHz, CDCl₃, TMS) δ : 4.05 (t, 2H), 1.70 (m, 2H), 1.37 (m, 2H), 0.96 (t, 3H). ¹³C NMR (100.5 MHz, CDCl₃, TMS) δ : 185.20, 154.99 (s), 43.60, 29.81, 19.85 (s), 13.53. Anal. calcd. (%): C 45.68, H 6.27, N 9.69; found: C 46.80, H 7.01, N 9.86.

X-ray crystallography

Crystal data for 3e^{Et}: C₇H₁₀N₂O₂Se, fw 233.13, orthorhombic, space group *P*2₁2₁2₁ (no. 19), *a* = 5.249(1), *b* = 10.406(3), *c* = 16.647(1) Å, *U* = 909.3(3) Å³, *Z* = 4, μ (Mo–K α) = 40.48 cm⁻¹, ρ_{calc} = 1.703 g cm⁻³; 1721 reflections measured, 1580 unique (*R*_{int} = 0.018). Intensity data were collected at room temperature with an Enraf–Nonius CAD4 diffractometer using graphite-monochromatised Mo–K α radiation. Lorentz, polarization, and a semiempirical absorption correction (41) were applied to all the data. The structure was solved by direct methods (MULTAN) (42) and refined by full-matrix least-squares with anisotropic displacement parameters for all the non-hydrogen atoms. The final *R* and *R*_w indices were 0.030 and 0.044 for 1339 reflections with *I* > 3 σ (*I*). All H atoms were seen in difference Fourier maps, but not refined. Sources of neutral atomic scattering factors for all atoms are given in ref. (43). Anomalous dispersion effects were included in *F*_c; and the values for $\delta f'$ and $\delta f''$ were those of ref. (44). All the calculations were performed using Personal SDP software (45, 46). Atomic coordinates, displacement parameters, bond lengths and angles have been deposited as supplementary material and may be purchased from the Depository of Unpublished Data, Document Delivery, CISTI, National Research Council Canada, Ottawa, ON K1A 0S2 (http://www.nrc.ca/cisti/docdel/order_electronic_e.shtml) for information on ordering

electronically). This material has also been deposited with the Cambridge Crystallographic Data Centre. Copies of the data can be obtained, free of charge, on application to the Director, CCDC, 12 Union Road, Cambridge CB2 1EZ, U.K. (Fax: 44-1223-336033 or e-mail: deposit@ccdc.cam.ac.uk).

Computations

Quantum chemical calculations were carried out using the commercially available suite of programs Gaussian 94 (47). Density functional calculations (16, 17) (DFT) were performed using the hybrid BECKE3LYP functional (which uses a mixture (22) of Hartree–Fock and DFT exchange along with DFT correlation: the Lee–Yang–Parr correlation functional together with the Becke’s gradient correction) (23), Schafer, Horn, and Ahlrichs’ (24) pVDZ basis set for C, H, N, O, S, and Se were used for all calculations. Numerical integration was performed using the FineGrid option, which indicates that a total of 7 500 points are used for each atom. After a geometry optimization performed starting from structural data (where available) regularized to satisfy the C_{2v} symmetry, harmonic frequencies were obtained using the second derivatives of the DFT energy, computed by numerical differentiation of the DFT energy gradients. Finally NBO (29) calculations have been performed for each molecule using the converged density matrix corresponding to the equilibrium geometries. All point group representations refer to the model molecules disposed on the *xy* plane with the C(1)=X bond lying on the *y* axis. Calculations have been performed on an IBM Risc 6000 550H, DECServer 4000, and on a VAIER Intel Pentium III 450 MHz Personal Computer running Linux.

Acknowledgments

The project was carried out as a part of the “Progetto Finalizzato Materiali Speciali per Tecnologie Avanzate II” of the “Consiglio Nazionale delle Ricerche.” We wish to acknowledge the Advanced Materials Laboratory (LaMI) under the auspices of the European Union and Regione Basilicata for financial support. We also wish to thank Dr. Francesco Usai for help in the synthesis.

Supporting information

Table S1, giving details of the data collection and refinement, atomic coordinates, displacement parameters, bond lengths and angles for 3e^{Et}. Optimized geometries in Cartesian coordinate form and frontier Kohn–Sham orbital energies at the BECKE3LYP level for all compounds reported in Scheme 3.

References

1. F.A. Devillanova and G. Verani. *Aust. J. Chem.* **33**, 279 (1980).
2. F.A. Devillanova and G. Verani. *Tetrahedron*, **37**, 1803 (1981).
3. H. Biltz and E. Topp. *Chem. Ber.* **46**, 1401 (1913).
4. M. Ponomareff. *Bull. Soc. Chim. Fr.* **18**, 97 (1872).
5. P. Brix and J. Voss. *J. Chem. Res. Miniprint*, **8**, 2218 (1993).
6. H. Brederbeck. *Chem. Ber.* **101**, 1863 (1968).

7. H.W. Roesky, H. Hofman, W. Clegg, M. Noltemeyer, and G.M. Sheldrick. *Inorg. Chem.* **21**, 3798 (1982).
8. A.C. Fabretti, G.C. Franchini, C. Preti, and G. Tosi. *Can. J. Chem.* **55**, 344 (1977).
9. D. Atzei, F. Bigoli, P. Deplano, M.A. Pellinghelli, and E.F. Trogu. *Phosphorus Sulfur Relat. Elem.* **37**, 189 (1988).
10. F. Bigoli, P. Deplano, F.A. Devillanova, J.R. Ferraro, V. Lippolis, P.J. Lukes, M.L. Mercuri, M.A. Pellinghelli, and E.F. Trogu. *Inorg. Chem.* **36**, 1218 (1997).
11. M.C. Aragoni, M. Arca, F. Demartin, F.A. Devillanova, A. Garau, F. Isaia, F. Lejl, V. Lippolis, and G. Verani. *J. Am. Chem. Soc.* **121**, 7098 (1999), and refs. therein.
12. S. Sheibe, B.J. Pedersen, and S.-O. Lawesson. *Bull. Soc. Chim. Belg.* **87**, 229 (1978).
13. F. Bigoli, P. Deplano, F.A. Devillanova, V. Lippolis, P.J. Lukes, M.L. Mercuri, M.A. Pellinghelli, and E.F. Trogu. *J. Chem. Soc. Chem. Commun.* 371 (1995).
14. M. Arca, F. Demartin, F.A. Devillanova, A. Garau, F. Isaia, F. Lejl, V. Lippolis, S. Pedraglio, and G. Verani. *J. Chem. Soc. Dalton Trans.* 3731 (1998).
15. F. Bigoli, P. Deplano, S. Marcis, M.L. Mercuri, R. Onnis, G. Orrù, M.A. Pellinghelli, and E. F. Trogu. *Phosphorus Sulfur Silicon Relat. Elem.* **659**, 136 (1998).
16. J. Labanowsky and J. Andzelm. *Density functional methods in chemistry.* Springer-Verlag, New York. 1991.
17. E.S. Kryachko and E.V. Ludeña. *Energy density function theory of many electron systems.* Kluwer Academic Publisher, NL. 1990.
18. D.L. Klayman and R.J. Shine. *J. Org. Chem.* **34**, 3549 (1969).
19. D.R. Davies and J.J. Blum. *Acta Crystallogr.* **8**, 129 (1955).
20. X.M. He, S. Swaminathan, B.M. Craven, and R.K. McMullan. *Acta Crystallogr. Sect. B: Struct. Sci.* **B44**, 271 (1988).
21. B.M. Craven and R.K. McMullan. *Acta Crystallogr. Sect. B: Struct. Crystallogr. Cryst. Chem.* **B35**, 934 (1979).
22. A.D. Becke. *J. Chem. Phys.* **98**, 1372 (1993).
23. C. Lee, W. Yang, and R.G. Parr. *Phys. Rev. B Condens. Matter Mater. Phys.* **37**, 785 (1988).
24. A. Schafer, H. Horn, and R. Ahlrichs. *J. Chem. Phys.* **97**, 2571 (1992).
25. H.-K. Fun, N. Janarthanan, K. Ramadas, A. Ramnathan, K. Sivakumar, and K. Subramanian. *Acta Crystallogr. Sect. C: Cryst. Struct. Commun.* **C51**, 2446 (1995).
26. F.H. Allen, O. Kennard, D.G. Watson, L. Brammer, G. Orpen, and R. Taylor. *J. Chem. Soc. Perkin Trans 2*, **1987**, S1.
27. T.A. Koopmans. *Physica*, **1**, 104 (1933).
28. J.L. Meeks and S.P. McGlynn. *J. Am. Chem. Soc.* **97**, 5079 (1975).
29. A.E. Reed, L.A. Curtiss, and F. Weinhold. *Chem. Rev.* **88**, 899 (1988).
30. F. Jensen. *Introduction to computational chemistry.* John Wiley, Chichester, U.K. 1999. pp. 229–233.
31. F.A. Devillanova and G. Verani. *J. Heterocycl. Chem.* **16**, 945 (1979).
32. F.A. Devillanova and G. Verani. *Tetrahedron*, **35**, 511 (1979).
33. F.A. Devillanova and G. Verani. *Tetrahedron*, **37**, 1803 (1981).
34. I. Cau, F. Cristiani, F.A. Devillanova, and G. Verani. *J. Chem. Soc. Perkin Trans. 2*, 759 (1985).
35. F. Cristiani, F.A. Devillanova, A. Garau, F. Isaia, V. Lippolis, and G. Verani. *Heteroat. Chem.* **5**, 65 (1994).
36. M.C. Aragoni, M. Arca, F.A. Devillanova, A. Garau, F. Isaia, V. Lippolis, and G. Verani. *Coord. Chem. Rev.* **184**, 271 (1999).
37. G. Carta and G. Crisponi. *Tetrahedron*, **37**, 2115 (1981).
38. G. Carta and G. Crisponi. *J. Chem. Soc. Perkin Trans. 2*, 53 (1982).
39. L. Coclers, A. Vanclef, and R. Bouché. *Spectrosc. Lett.* **11**, 799 (1978).
40. G. Rauhut and P. Pulay. *J. Phys. Chem.* **99**, 3093 (1995).
41. A.C.T. North, D.C. Phillips, and F.S. Mathews. *Acta Crystallogr. Sect. A: Cryst. Phys. Diffr. Theor. Gen. Crystallogr.* **A24**, 351 (1968).
42. P. Main, S.J. Fiske, S.E. Hull, L. Lessinger, G. Germain, J.P. Declercq, and M.N. Wolfson. *MULTAN 80*, Universities of York, England and Louvain, Belgium. 1980.
43. D.T. Cromer and J.T. Waber. *International tables for X-ray crystallography. Vol. IV.* The Kynoch Press, Birmingham, U.K. 1974. Table 2.2B. p. 1990.
44. D.T. Cromer. *International tables for X-ray crystallography. Vol. IV.* The Kynoch Press, Birmingham, U.K. Table 2.3.1. 1974.
45. B. Frenz. *Comput. Phys.* **2**, 42 (1988).
46. B. Frenz. *Crystallographic computing 5. Ch. 11.* Oxford University Press, Oxford, U.K. 1991. pp. 126–135.
47. Gaussian 94 (Revision D.1 & E.1), M.J. Frisch, G.W. Trucks, H.B. Schlegel, P.M.W. Gill, B.G. Johnson, M.A. Robb, J.R. Cheeseman, T.A. Keith, G.A. Petersson, J.A. Montgomery, K. Raghavachari, M.A. Al-Laham, V.G. Zakrzewski, J.V. Ortiz, J.B. Foresman, C.Y. Peng, P.Y. Ayala, M.W. Wong, J.L. Andres, E.S. Replogle, R. Gomperts, R.L. Martin, D.J. Fox, J.S. Binkley, D.J. Defrees, J. Baker, J.P. Stewart, M. Head-Gordon, C. Gonzalez, and J.A. Pople. *Gaussian, Inc., Pittsburgh, Pa.* 1995.